RESEARCH PAPER

PCCP
www.rsc.org/pccp

Ultrafast transient lens spectroscopy of various C_{40} carotenoids: lycopene, β-carotene, (3*R*,3′*R*)-zeaxanthin, (3*R*,3′*R*,6′*R*)-lutein, echinenone, canthaxanthin, and astaxanthin†

Matthäus Kopczynski,[a] Thomas Lenzer,*[ab] Kawon Oum,*[a] Jaane Seehusen,[a] Marco T. Seidel[a] and Vladimir G. Ushakov[a]

[a] *Institut für Physikalische Chemie, Universität Göttingen, Tammannstrasse 6, D-37077 Göttingen, Germany. E-mail: tlenzer@gwdg.de; koum@gwdg.de; Fax: +49 551 39 12598; Tel: +49 551 39 3150*

[b] *Max-Planck-Institut für biophysikalische Chemie, Abt. Spektroskopie und Photochemische Kinetik (10100), Am Fassberg 11, D-37077 Göttingen, Germany. Fax: +49 551 201 1501; Tel: +49 551 201 1344*

Received 10th May 2005, Accepted 10th June 2005
First published as an Advance Article on the web 21st June 2005

The ultrafast internal conversion (IC) dynamics of seven C_{40} carotenoids have been investigated at room temperature in a variety of solvents using two-color transient lens (TL) pump–probe spectroscopy. We provide comprehensive data sets for the carbonyl carotenoids canthaxanthin, astaxanthin, and—for the first time—echinenone, as well as new data for lycopene, β-carotene, (3*R*,3′*R*)-zeaxanthin and (3*R*,3′*R*,6′*R*)-lutein in solvents which have not yet been investigated in the literature. Measurements were carried out to determine, how the IC processes are influenced by the conjugation length of the carotenoids, additional substituents and the polarity of the solvent. TL signals were recorded at 800 nm following excitation into the high energy edge of the carotenoid S_2 band at 400 nm. For the S_2 lifetime solvent-independent upper limits on the order of 100–200 fs are estimated for all carotenoids studied. The S_1 lifetimes are in the picosecond range and increase systematically with decreasing conjugation length. For instance, in the sequence canthaxanthin/echinenone/β-carotene (13/12/11 double bonds) one finds $\tau_1 \approx 5$, 7.7 and 9 ps for the $S_1 \rightarrow S_0$ IC process, respectively. Hydroxyl groups not attached to the conjugated system have no apparent influence on τ_1, as observed for canthaxanthin/astaxanthin ($\tau_1 \approx 5$ ps in both cases). For all carotenoids studied, τ_1 is found to be insensitive to the solvent polarity. This is particularly interesting in the case of echinenone, canthaxanthin and astaxanthin, because earlier measurements for other carbonyl carotenoids like, *e.g.*, peridinin partly showed dramatic differences. The likely presence of an intramolecular charge transfer state in the excited state manifold of C_{40} carbonyl carotenoids, which is stabilized in polar solvents, has obviously no influence on the measured τ_1.

1. Introduction

Carotenoids play a key role in photosynthetic systems, where they serve as light-harvesting pigments in the blue–green spectral region.[1] Lycopene, for instance, acts as an efficient donor in the light-harvesting complexes of purple bacteria.[2] Antenna systems associated with Photosystem II in green plants contain, *e.g.*, β-carotene, lutein, zeaxanthin (Fig. 1), violaxanthin, antheraxanthin, and neoxanthin.[3] Carotenoids also protect against excessive light by quenching both singlet and triplet states of bacteriochlorophylls.[4]

In addition, they are known as efficient antioxidants, which are of great importance for human health.[5] Zeaxanthin and lutein are present in high concentrations in the yellow spot of the human retina and are probably involved in the photoprotection of the human eye.[6] For these reasons carotenoids are of great importance in the food industry (also as coloring agents) and therefore produced synthetically on an industrial scale.[7] Fig. 1 contains structures for the C_{40} carotenoids studied in this work. In the following, we adopt a nomenclature following Polivka and Sundström,[1] where the conjugation of the carotenoids is abbreviated as *N*β*j*O*k*: *N* is the number of conjugated C=C bonds in the carotenoid backbone, β*j* denotes an extension of this conjugation to *j* C=C bonds located at a terminal β-ionone ring, and O*k* means that the conjugation is extended to *k* carbonyl groups. This way, the following abbreviations are obtained: lycopene (11), β-carotene ("9β2"), (3*R*,3′*R*)-zeaxanthin ("9β2"), (3*R*,3′*R*,6′*R*)-lutein ("9β1"), echinenone ("9β2O1"), canthaxanthin ("9β2O2") and astaxanthin ("9β2O2").

The simplest model of carotenoid photophysics consists of three states: Their strong absorption in the blue–green region ($\varepsilon \approx 10^5$ L mol^{-1} cm^{-1}) is due to the one-photon transition from the S_0 state ($^1A_g^-$) to the S_2 state ($^1B_u^+$), where labels are based on idealized C_{2h} symmetry. In contrast, the one-photon transition to the S_1 state ($^1A_g^-$) is symmetry forbidden (though two-photon excitation is possible[8,9]). A variety of time-resolved spectroscopic techniques have been applied to study the internal conversion (IC) and energy transfer processes in the S_2 and S_1 excited states, and the involvement of additional intermediate states in the dynamics has been invoked for the interpretation of the results (see the excellent review by Polivka and Sundström[1] for more details). Very recent femtosecond stimulated Raman studies by Mathies and co-workers, however, seem to point towards a revival of the simple 3-state model, as the temporal evolution of their vibrational spectra is consistent with only two low-lying excited states (S_2 and S_1).[10]

† Electronic supplementary information (ESI) available: Absorption spectra of carotenoids in different solvents. See http://dx.doi.org/10.1039/b506574g

DOI: 10.1039/b506574g

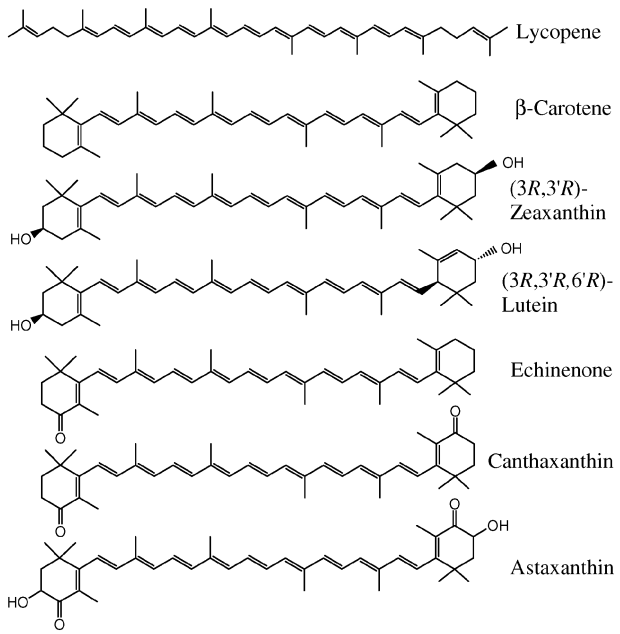

Fig. 1 C_{40} carotenoids investigated in this work.

They explain the ultrafast (sub-20-fs) Stokes shift observed in earlier excited-state absorption measurements[11] with a rapid initial nuclear relaxation out of the Franck–Condon region. Typically the $S_2 \rightarrow S_1$ IC process in the C_{40} carotenoids investigated so far is very fast (<200 fs), whereas the $S_1 \rightarrow S_0$ IC occurs on the picosecond timescale.[1]

The excited states of carbonyl carotenoids have unique properties which play an important role in light-harvesting complexes of algae.[12] One example is peridinin, which is the main light-harvesting pigment in the peridinin–chlorophyll-*a* protein complex. In nonpolar solvents, lifetimes of the peridinin S_1 state are *ca.* 170 ps, whereas in polar environments they are reduced to about 10 ps.[13,14] Currently these findings are interpreted in terms of a combined S_1/ICT (intramolecular charge transfer state), for which polar solvents stabilize a structure, where electron density is transferred from the polyene chain to the C=O group. However, the model has not yet been able to explain the polarity dependence of the lifetime of the S_1/ICT state.[15] While other carbonyl carotenoids show a behavior similar to peridinin, our current study will demonstrate, that the C=O containing C_{40} carotenoids investigated in this work exhibit essentially no solvent dependence, in agreement with two very recent studies employing time-resolved transient absorption (TA).[16,17] This raises further questions about the nature of the electronic states of these systems.

Although not involved in photosynthetic processes, astaxanthin (Fig. 1) is a particularly interesting system, because it is incorporated in the β-crustacyanin protein complex. The interaction causes a large 160 nm red shift relative to its spectrum in solution.[18] This can be explained by strong exciton coupling between two astaxanthins in close proximity.[17,19] The observed reduction of the S_1 state lifetime in the protein complex by about a factor of three compared with astaxanthin in solution[17] is probably due to the fact that the protein establishes hydrogen bonds with the two carbonyl groups of astaxanthin, and forces the terminal rings into a coplanar structure with the rest of the conjugated backbone. This extends the effective conjugation length considerably.[18,20] Studies of the excited states in simple environments, like solvents of different polarity, are certainly helpful for understanding such specific carotenoid–protein interactions. As another example of interest to the current study, 3′-hydroxyechinenone is incorporated in the orange carotenoid protein present in specific cyanobacteria, which is possibly involved in photoprotection.[21] The lifetime of the S_1 state in the protein environment is considerably shorter than in solution.[16] All these studies make clear, that additional investigations of structurally different carbonyl carotenoids in simple and complex environments are necessary to understand the photophysical properties and the dynamics of these systems in their S_1 and S_2 states. The present study of astaxanthin and related carbonyl carotenoids such as canthaxanthin and echinenone in a variety of solvents is intended as one step in this direction.

2. Transient lens spectroscopy

In this paper, we apply transient lens (TL) spectroscopy to characterize the internal conversion dynamics of the carotenoids in detail. The applicability of such a setup has been demonstrated earlier for β-carotene in *n*-hexane by Sawada and co-workers.[22] The principle of the technique is shown in Fig. 2. Two laser beams (pump and probe) are focused by a lens into a cuvette containing the solution of interest. The cuvette is movable along the Z direction between the lens and detector. In the following example, however, we keep the cuvette in front of the lens focus (prefocal position). A photodiode with a very small light-sensitive area is positioned in the far field (alternatively an arrangement of a larger area detector with a pinhole can be used). The pump laser beam with Gaussian intensity distribution promotes solute molecules (index of refraction n_0) to an excited electronic state, which is assumed to have a larger index of refraction $n_0 + \Delta n$ ($\Delta n > 0$, see Fig. 2(A)). Because of the Gaussian intensity distribution of the pump beam, $n_0 + \Delta n$ will be larger in the center than at the edges, which leads to the formation of a *transient convex lens*. The second (= probe) beam is then focused into the cuvette. Without the pump laser the probe beam would diverge to a diameter given by the dotted arrows in Fig. 2(A). However, because of the additional transient convex lens the beam is widened up further (solid arrows), and the detector records a reduced intensity. Because the electronically excited molecules in the solution will eventually relax back to the ground state, the transient lens will disappear with a time constant characteristic for the relaxation process, and the intensity at the detector will go back to the level before the experiment. A schematic intensity trace of the TL process is given on the right side. Analogously, as shown in Fig. 2(B), if the excited electronic state has a smaller index of refraction $n_0 + \Delta n$ than the ground state ($\Delta n < 0$), a *transient concave lens* is formed inside

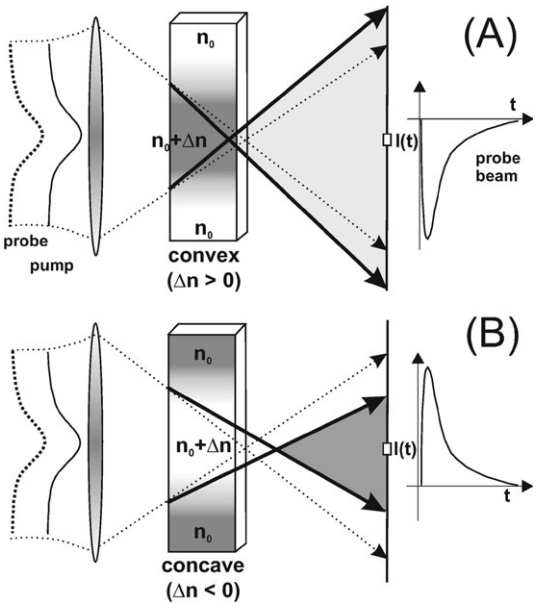

Fig. 2 Principle of transient lens signal formation.

the cuvette. Correspondingly, an intensity maximum is observed at the detector, see the intensity time trace on the right side. Note that the sign of the effect depends on the position of the cuvette. If it was located behind the lens focus (postfocal position), the observed intensity profiles would exactly change around. In fact, by scanning the cuvette along the Z-direction at a specific pump–probe time delay, one can observe this sign change with an intermediate zero crossing.[23–25] More details of these "Z-scan" measurements will be given in Section 4.2.

Lens phenomena have been known for a long time, and different types of lenses can occur:[26] On the nanosecond to millisecond time scale lenses are produced by heating (thermal lens)[27] or electrostriction (diffusion into the region of an intense laser field). On a much faster time scale (pico- to femtoseconds) the latter nonlocal effects are not important any more, and other types of lenses dominate. Most relevant to our investigations are *"population lenses"*,[22] which occur when a change in the electronic state of a molecule is accompanied by a change of its refractive index. This allows us to track the population transfer of carotenoid molecules due to IC from S_2 *via* S_1 to S_0. Note, that the TL method is therefore sensitive to electronic population transfer, *i.e.*, the IC time constants in the case of the carotenoids. Superimposed vibrational energy transfer processes within one electronic state will not influence the signal, which is an advantage, *e.g.*, over TA techniques. On the other hand a fully analyzed set of TA signals at different probe wavelengths can provide valuable complementary information on vibrational relaxation processes and spectral band shifts. A technical advantage of the TL technique is that it does not require a specific absorption band for probing the molecular dynamics, because only the change in the real part of the refractive index needs to be monitored. This simplifies the experimental setup considerably. In addition, it is to be hoped that future analysis of the relative refractive index changes between the different electronic states, as probed by TL spectroscopy, might yield additional information on their dipole moments.

Besides population changes, nonlinear effects like the optical Kerr effect (OKE) are also known to produce lens phenomena on the ultrafast time scale.[28,29] The index of refraction can be expressed in terms of the nonlinear index n_2

$$n = n_0 + \frac{n_2}{2}|E|^2 = n_0 + \Delta n \qquad (1)$$

where n_0 is the linear index of refraction and E is the peak electric field of the laser beam within the sample. The slower "nuclear" component of the OKE due to molecular reorientation of the carotenoid molecules is not affecting our lens signal, because reorientation times of these molecules are expected to be slow compared with the IC dynamics of our systems.[30] However, fast "electronic" components contribute to our signals, with n_2 and $\Delta n > 0$ in eqn. (1). These originate from the solvent and (to a very small extent) from the windows of the quartz cuvette, for details see Section 4.1. Finally, two other lens effects must be mentioned, which however do not play a role in our case:[26] "Molecular interaction lenses" due to OKE contributions at high concentrations can be neglected, as shown by our concentration dependent experiments (Section 4.1.). Also lenses originating from a volume change of the solvent are not present in our case, because they require a fast and pronounced change of the solute geometry.

In the following we will describe our transient lens setup, and then present our results on the dynamics of several C_{40} carotenoids with and without carbonyl groups, including the first measurements for echinenone.

3. Experimental

Fig. 3 schematically illustrates the experimental setup for the transient lens and Z-scan experiments. A mode-locked Ti : sapphire laser (Spectra-Physics Tsunami) pumped by a Nd : YVO_4 laser (Spectra-Physics Millenia Xs) generated pulses at 800 nm with a repetition rate of 82 MHz and an average laser power of about 1.5 W. The laser beam was split into two parts by a dichroic mirror. One part was sent through an acousto-optic modulator (AOM), which was operated at a frequency of 2 MHz by means of a pulse generator, and subsequently frequency-doubled in a LBO crystal to generate an intensity-modulated 400 nm pump beam with pulse energies <0.1 nJ. The other part was used as probe beam (typical energy <1 nJ pulse^{-1}) and was time-delayed using a motorized computer-controlled delay line. The time resolution was typically about 130 fs, as estimated from cross-correlation measurements of the 400 nm and 800 nm beams in a BBO crystal. The pump and probe pulses, having approximately Gaussian intensity profiles, were recombined in a collinear beam-in-beam arrangement, with the polarization set to parallel. The pulses were then sent through a quartz lens (Suprasil I, $f = 50$ mm) and focused into a flow cuvette (Suprasil I, path length 1 mm) which was mounted on a linear translation stage and contained the carotenoid solution of interest. Its entrance window surface was aligned perpendicularly with respect to the incoming beams. In the TL experiments the cuvette was accurately positioned in front of the focus to optimize the signal. Dual-beam two-color Z-scans were measured by recording the lens signal of the solution at different distances Z with respect to the focal plane for a specific pump–probe delay time. TL and Z-scan signals were detected by a sensitive avalanche photodiode (APD, 200 μm active diameter) in the far field. Because of its small diameter the APD monitors only a small center area of the complete beam. Note that this arrangement is equivalent to a standard setup employing a larger area detector with an aperture.[29] The pump beam was cut off in front of the APD by an appropriate combination of color and neutral density filters, so that the recorded intensity change was only due to the time-dependent divergence of the probe beam. The resulting signal was fed into a lock-in amplifier which used the 2 MHz modulation of the pulse generator as its reference signal. The lock-in-signal was then transferred to a PC running an Agilent VEE program which handled the signal acquisition using an A/D converter card and the control of the delay line *via* a GPIB interface.

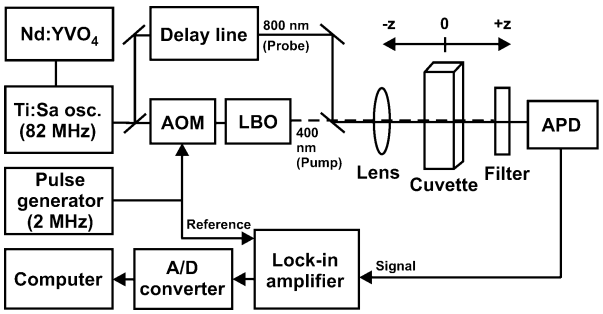

Fig. 3 Experimental two-color pump–probe transient lens setup.

The highly purified carotenoid samples were generously provided by BASF AG. Lycopene, β-carotene, (3R,3′R)-zeaxanthin, echinenone, canthaxanthin, and astaxanthin were all in their *all-trans* (*all-E*) configuration with purity >97%. (3R,3′R,6′R)-Lutein had a purity of better than 95% [*all-trans* (*all-E*)], with a remaining impurity of mainly (3R,3′R)-zeaxanthin (<5%). The astaxanthin samples were a statistical mixture with a (3R,3′R) : (3S,3′S) : (3R,3′S-*meso*) ratio of 1 : 1 : 2. All solvents had a purity ≥ 99%. Typically a concentration of about 2×10^{-4} M was used, and the shape of the signals and the extracted time constants were the same when the concentration was reduced by about two orders of magnitude (see below). The raw transient lens signal also contained

some contributions which were due to the optical Kerr effect (OKE) of the pure solvent and transient absorption (TA) of the carotenoid. The former one was detected by recording the transient lens signal for the pure solvent. The absorption contribution was quantified by placing an additional quartz lens (Suprasil I, $f = 30$ mm) in front of the detector, so that the complete probe beam intensity transmitted by the solution was detected on the APD. A detailed discussion of extracting the "pure" TL signal will be given in the following section.

4. Results

4.1 Extraction of the pure carotenoid TL signal

Fig. 4(A) shows a typical experimental raw TL signal for β-carotene in acetone. The signal first decays slightly, and then rises. Subsequently, the signal decays sharply to negative values, and this negative signal finally decays to zero. The slope of the first three components is steep and only upper limits for the time constants of the processes involved can be given, whereas the final decay of the negative signal towards zero is well-resolved so that an accurate time constant can be deduced (see below). It is evident that several processes beside the carotenoid TL signal must contribute to this complicated shape, and we will quantify these independently in the following.

The first dip in the raw signal is due to a superposition of two processes: an ultrafast "electronic" optical Kerr response of the solvent and transient absorption (TA) from the carotenoid S_2 state. OKE solvent contributions of this type have also been observed in previous studies.[22,28] We recorded the Kerr signal of the pure solvent separately under the same experimental conditions as the raw signal. It is shown in Fig. 4(B). The solvents all possess a positive n_2 value for the nonlinear index of refraction which results in a transient convex OKE lens. Because the cuvette in our experiments is typically positioned in front of the focus of the quartz lens (compare Fig. 2), the OKE introduces an additional divergence at the detector, which results in a negative signal, as observed in Fig. 4(B). The shape of the OKE is solvent dependent, and varies between either a symmetric Gaussian-like or a more or less asymmetric appearance due to an additional small pedestal towards larger pump–probe times. We also detected a very small symmetric ultrafast OKE contribution around zero delay time, which originated from the windows of the empty cuvette. Its amplitude is, however, negligible. These types of signals are well-known for dielectric window materials.[25]

In addition, we have observed TA features for all the carotenoids considered in this study. These can be separately measured by introducing an additional focusing lens in front of the detector in order to collect the whole transmitted intensity of the probe beam. An example is shown in Fig. 4(C). Because of the good sensitivity of the high modulation frequency lock-in detection technique used in this study, even very small absorption changes (typically 0.01% of total intensity) will give rise to an appreciable signal. Although no strong features of transient carotenoid absorption bands are observed around 800 nm,[31] we nevertheless believe that we are detecting a weak excited-state absorption (ESA) originating from the initially prepared S_2 state (possibly including some smaller contributions of higher excited electronic states). This interpretation is supported by the transient pump–probe spectra of Cerullo *et al.* for β-carotene,[11] which are consistent with a weak absorption signal in this spectral region at very short times. The S_2 state decays to the S_1 state *via* internal conversion, and this process manifests itself in the sharp decay of the negative TA signal to zero in Fig. 4(C). In fact, for some of the carotenoids we see a subsequent—yet almost negligible—negative pedestal which slowly decays towards zero [barely visible in Fig. 4(C) at longer times]. This is most likely due to an extremely weak S_1 excited-state absorption which decays with the IC time constant for $S_1 \rightarrow S_0$, (possibly including some superposition of vibrational energy transfer processes[1]). The signal amplitude is too small to allow for a reliable estimate of this time constant. For the ultrafast $S_2 \rightarrow S_1$ IC process we can typically give an upper limit of 150–200 fs. The ultrafast S_2 decay times we observe, are consistent with known decay times of the S_2 state obtained after excitation at lower energies.[32]

To obtain the "pure" TL signal of the carotenoids the solvent Kerr and TA contributions were appropriately subtracted from the raw signal (see Section 4.2.). The result for β-carotene in acetone is shown in Fig. 4(D). The shape of the signal is characteristic for all the carotenoids investigated in this work, compare, *e.g.*, the time trace for the carbonyl carotenoid canthaxanthin dissolved in tetrahydrofuran (THF) shown in Fig. 5. The fast rise within the time-resolution

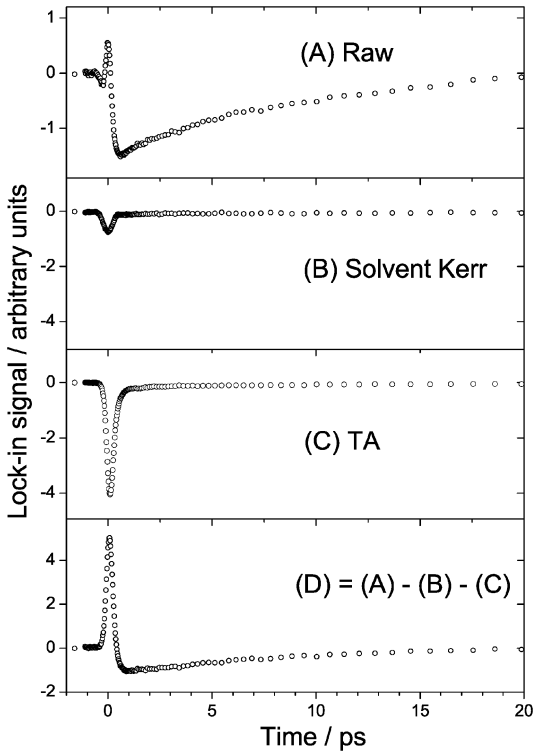

Fig. 4 Extraction of the pure TL signal (D) by subtracting the Kerr response of the solvent (B) and the transient absorption contribution (C) from the raw signal (A). System: β-Carotene in acetone.

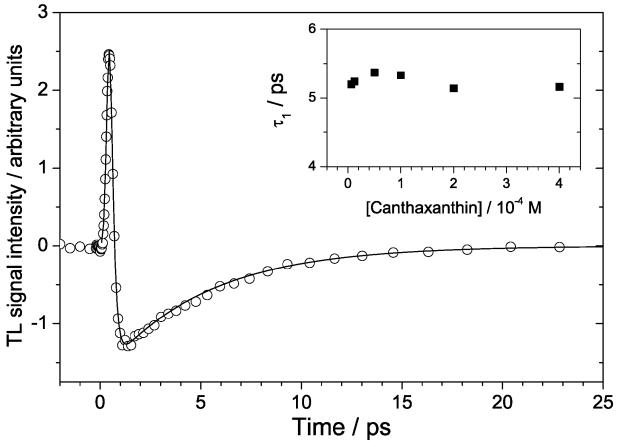

Fig. 5 Transient lens signal of canthaxanthin in tetrahydrofuran. ○: experiment; solid line: best fit as described in the text. Inset: lifetime τ_1 for the $S_1 \rightarrow S_0$ internal conversion process as a function of the concentration of canthaxanthin in tetrahydrofuran.

of our setup is due to the initial preparation of the S_2 state by the pump beam. It decays very quickly to negative values. We attribute the latter process to ultrafast IC from S_2 to S_1 (time constant τ_2), in accordance with earlier experimental results.[22,32] The negative signal finally decays to zero on a slower timescale, which is attributed to IC from S_1 to S_0. From this well-resolved final part of the signal accurate time constants for the $S_1 \rightarrow S_0$ transition can be determined. The time constants τ_1 and τ_2 for the two IC processes were extracted from the TL curves by fitting a sum of two exponentials for the two IC processes, which was convoluted with the cross-correlation of our laser pulses, to the experimental signal using a Levenberg–Marquardt algorithm.

The sign changes in the TL signal also allow us to determine the relative order of the respective refractive indices of the three electronic states involved. Because a negative signal with prefocal position of the cuvette corresponds to a convex transient lens, the relative order must be $n(S_1) > n(S_0) > n(S_2)$.

In addition, we tested the dependence of the TL signal on carotenoid concentration and the energy of the pump and probe lasers. All were linear and no distortions of the TL signal were observed. An example for the concentration dependence of the extracted time constant τ_1 of the internal conversion $S_1 \rightarrow S_0$ is shown in the inset of Fig. 5 for canthaxanthin in tetrahydrofuran. It is clear that there is essentially no variation of τ_1 for a roughly 100 fold increase of the concentration from 6×10^{-6} to 4×10^{-4} M, and values between 5.2 and 5.3 ps are obtained.

4.2 *Z*-scans

Additional information on the refractive index changes in our signals can be gathered by the *Z*-scan technique, which has been applied *e.g.* to the measurement of thermal lenses and nonlinear effects.[23–25,33] Z denotes the position of the sample between the focusing lens and the detector, with $Z = 0$ being the focal position (Figs. 2 and 3). Scanning the position of the sample (in our case the carotenoid solution inside the flow cuvette) along the *Z*-axis gives rise to characteristic changes of the light intensity recorded on a detector behind an aperture placed in the far field. Single- and dual-beam arrangements of the technique have been used.[25,33] For instance, *Z*-scans allow the determination of the sign, magnitude and order of the response of nonlinear-optics materials, where sensitivities are competitive with those of experimentally more complex methods, like *e.g.*, nonlinear interferometry and degenerate four-wave mixing.[24] Among others, semiconductors[34] and polymethine dyes have been studied so far.[35,36]

Fig. 6 shows our *Z*-scans for β-carotene in *n*-heptane. The laser beam travels from negative to positive Z, and the photodiode detector is located in the far field at large Z. The open circles correspond to a "closed-aperture (CA)" *Z*-scan, *i.e.* the "aperture" is given by the active diameter of the photodiode (200 μm). In this case a fixed pump–probe delay of $\Delta t = 1$ ps was used, which is located on the early part of the final slow component, see *e.g.*, Fig. 4(D). The "negative" intensity of the lens signal in this region corresponds to a reduction of the signal for S_1 relative to S_0 carotenoid molecules. Because in Fig. 4(D) the sample is in a prefocal position, a "convex" lens must be present, and the order of the refractive indices is $n(S_1) > n(S_0)$. The *Z*-scan in Fig. 6 is therefore characterized by a prefocal transmittance minimum (valley) and a postfocal transmittance maximum (peak).[25] The observed valley-peak distance (2.5 mm) corresponds to a beam waist of about 20 μm, which is consistent with our experimental conditions (laser beam diameter $d = 2$ mm and focal length of the lens $f = 50$ mm). The slight enhancement of the valley with respect to the peak is due to a small absorption superimposed on the raw signal, as mentioned above.

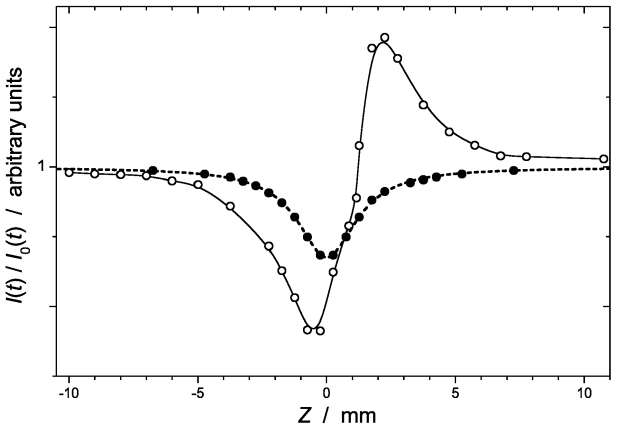

Fig. 6 Two-color *Z*-scans for β-carotene in *n*-heptane. ○: Detection with avalanche photodiode (APD) only, having 200 μm active diameter (corresponding to a "closed aperture" *Z*-scan), pump–probe delay 1.0 ps; ●: with an additional quartz lens in front of the APD, which mildly focuses the complete probe beam diameter on the active APD diameter (corresponding to an "open aperture" *Z*-scan), pump–probe delay 100 fs. Note that the latter setup is insensitive to lens effects.

The absorption contributions, *i.e.*, the imaginary part of the refractive index of the "carotenoid population lens" can be selectively obtained by an "open-aperture (OA)" *Z*-scan.[25] This is equivalent to our setup with an additional focusing lens for collecting the full diameter of the probe beam, as described above. The results are shown in Fig. 6 as filled circles. In this case a pump–probe delay of about 100 fs was used, which is located close to the minimum of the TA time trace in Fig. 4(C). Because the TA response is most likely due to excited state absorption from the S_2 state, the signal shows the expected pronounced minimum around $Z = 0$ and no sign change.

Indeed the different behavior of the lens (= population + OKE) and absorption signals with respect to the Z position of the cuvette is very convenient to separate their individual contributions to a CA signal ("Method I"). This is demonstrated in Fig. 7. If one performs a prefocal and a postfocal CA pump–probe experiment at symmetric positions $-Z$ and $+Z$ (left and right inset in Fig. 7), the transient absorption contribution (which has the same sign and magnitude in these locations, as shown in the OA *Z*-scan of Fig. 7) can be obtained *via*:[26]

$$I(t)_{TA} = 0.5 \cdot [I_{CA}(t)_{-Z} + I_{CA}(t)_{+Z}] \qquad (2)$$

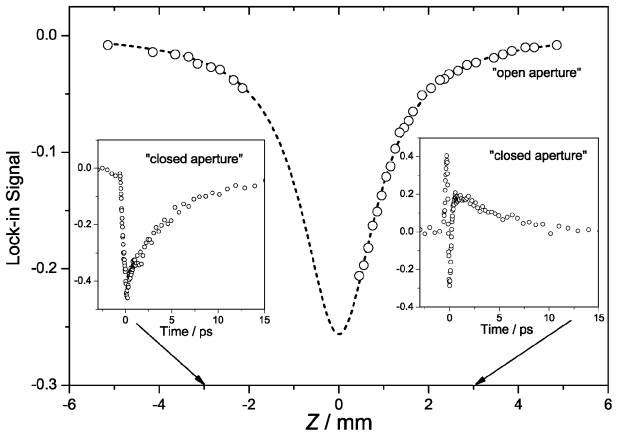

Fig. 7 Partial "open aperture" *Z*-scan for canthaxanthin in acetone at a pump–probe delay of 100 fs (○ and dashed fit line). The small insets show two raw signals (corresponding to "closed aperture" conditions) taken with the sample cuvette in a prefocal position ($Z = -3$ mm, left side) and a postfocal position ($Z = 3$ mm, right side).

In this case the lens contributions (having opposite sign) cancel out. In contrast, the TL plus OKE contribution is given by:[26]

$$I(t)_{\mathrm{TL\ +\ Kerr}}=0.5\cdot[I_{\mathrm{CA}}(t)_{-Z}-I_{\mathrm{CA}}(t)_{+Z}] \qquad (3)$$

where the absorption contributions (having the same sign) disappear. The Kerr lens contribution of the solvent can be removed by subtracting a "solvent-only" CA pump–probe experiment under the same conditions [$I_{\mathrm{CA}}(t)_{-Z,\mathrm{Kerr}}$] to obtain the pure TL signal $I(t)_{\mathrm{TL}}$.

There is also an alternative way to obtain the TL + Kerr contributions ("Method II"). One performs a CA pump–probe-experiment at a fixed Z position and subtracts an OA pump–probe trace at the same Z. In this case, a correct scaling factor for the OA signal is required prior to subtraction, because the absolute probe intensity I_0 at the photodiode is different for CA and OA measurements. Simply scaling by the ratio $I_{0,\mathrm{CA}}/I_{0,\mathrm{OA}}$, however, is not sufficient, because this would imply a uniform intensity distribution of the laser beam, whereas in reality this is approximately Gaussian. An additional "geometrical" scaling factor is therefore needed, which can be obtained by adjusting s in eqn. (4) so that agreement with eqn. (3) is obtained:

$$I(t)_{\mathrm{TL+Kerr}}=I_{\mathrm{CA}}(t)_{-Z}-I_{\mathrm{OA}}(t)_{-Z}\cdot I_{0,\mathrm{CA}}/I_{0,\mathrm{OA}}\cdot s \qquad (4)$$

We have found that s is typically 3.1 ± 0.4 under our experimental conditions. Again, the small Kerr lens contribution of the solvent can be removed by subtracting a time-resolved "solvent-only" CA pump–probe experiment under the same conditions [$I_{\mathrm{CA}}(t)_{-Z,\mathrm{Kerr}}$] to obtain the pure TL signal $I(t)_{\mathrm{TL}}$ of the carotenoid.

We tested "Method I" and "Method II" for the carotenoids canthaxanthin and β-carotene and found that eqns. (3) and (4) gave practically identical results. Note also that the time constants obtained from the fits are insensitive to the exact scaling factor used, even, *e.g.*, if s is varied by 30%. Because "Method II" is experimentally more convenient, we routinely used this approach for obtaining the TL signal.

4.3 Absorption spectra and lifetimes for the internal conversion processes of C_{40} carotenoids

Steady-state absorption spectra of the carotenoids were determined by us, and the complete set of spectra in all solvents (except for those shown in Fig. 8) can be found in the ESI.† The corresponding absorption maxima are given in Tables 1–3, as well as values from other sources where available.[37,38] We start with the results for the C_{40} carotenoids without a carbonyl group. The absorption spectrum of lycopene for $S_0 \rightarrow S_2$ exhibits a well-known three-peak-structure (spacing around 1350 cm^{-1}), whereas this structure for the other non-carbonyl carotenoids is not as pronounced and less well-resolved. The progression results from the combination of two symmetric vibrational stretching modes, C–C (1150 cm^{-1}) and C=C (1600 cm^{-1}). This partial loss of the peak structure is well-known and normally explained in terms of a broader distribution of conformers for species with β-ionone rings.[1]

(a) β-Carotene. Over the years β-carotene (conjugation: "9β2", see Fig. 1) has become a benchmark system for the investigation of carotenoid photophysics by various time-resolved pump–probe techniques, including transient absorption, fluorescence upconversion and Raman spectroscopy.[1,8,22,31,32,39–48] Therefore this well-known system is a good starting point for a comparison with the TL detection used in this work. Table 1 contains a list of lifetimes $\tau_1(S_1 \rightarrow S_0)$ and $\tau_2(S_2 \rightarrow S_1)$ for the IC processes of β-carotene in different solvents including the results from this work.

Because of the large amount of measurements in the literature, it necessarily represents only a subset of the available

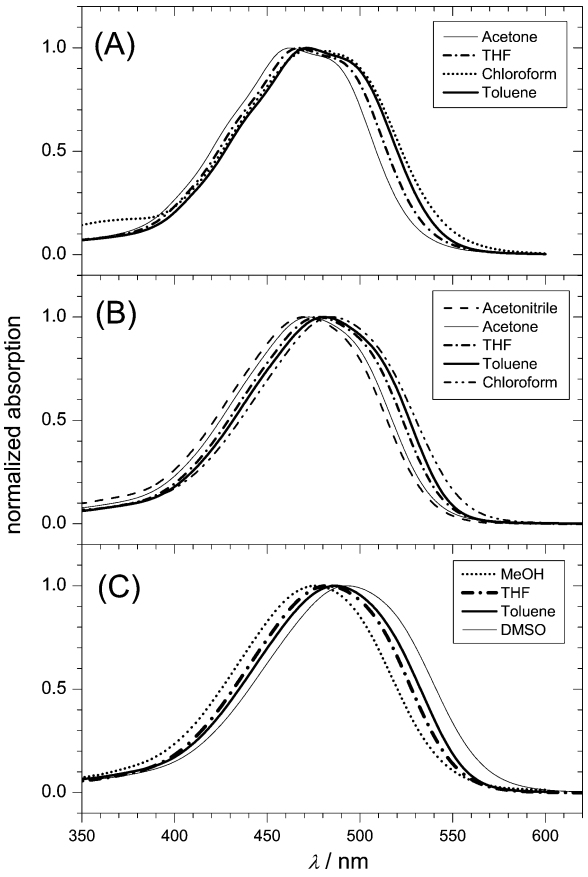

Fig. 8 Steady-state absorption spectra showing the different solvatochromic shifts of the $S_0 \rightarrow S_2$ band in various solvents: (A) echinenone, (B) canthaxanthin, and (C) astaxanthin.

data. For easier comparison, we also added the pump and probe wavelengths used in each experiment, the orientation polarizability Δf given by[49]

$$\Delta f=\frac{\varepsilon-1}{2\varepsilon+1}-\frac{n^2-1}{2n^2+1} \qquad (5)$$

as well as the absorption maximum for the $S_0 \rightarrow S_2$ transition. Here ε and n denote the dielectric constant and the index of refraction of the solvent, respectively. We find an excellent agreement of our τ_1 value in *n*-hexane of 9.0 ps with the earlier data of Billsten *et al.*[40] and van Grondelle and co-workers.[32] As in the earlier studies, our τ_1 values for β-carotene are practically insensitive to the solvent polarity, and are all close to 9 ps. Although we have a limited time resolution and small uncertainties related to the subtraction of the transient absorption peak around $t = 0$ we can nevertheless give a rough upper limit for the lifetime τ_2 of the $S_2 \rightarrow S_1$ IC process. Typical estimates are around 150 ± 50 fs. This is also in good agreement with most of the previously published data, as summarized in Table 1. Any fluctuations for the different solvents are due to slight variations of the temporal resolution of the experimental setup on a day-to-day level, as estimated by measurement of the cross-correlation function.

(b) Lycopene. For lycopene (conjugation: "11", Fig. 1) we observe considerably shorter lifetimes τ_1 than in the case of β-carotene, and values between 3.1 and 4.0 ps are found. These are in very good agreement with the data from earlier time-resolved studies (Table 2).[40,50–55] As for β-carotene no dependence on the solvent polarity can be found. Upper limits can be given for the lifetime τ_2 of the S_2 state, and typical values are around 150 fs.

Table 1 Lifetimes of β-carotene in various organic solvents: $\tau_1(S_1 \rightarrow S_0)$ and $\tau_2(S_2 \rightarrow S_1)$

Solvent	λ_{max}/nm	Δf	λ_{pump}/nm	λ_{probe}/nm	τ_1/ps	τ_2/fs	Method[g]	Ref.
n-Hexane	450[b]	0	475	470–650	9.1	140	TA	32
			449	~940	—	190	TA	39
				~1000	—	210		
			390	780	10	≤200	TL	22
			490	484	9.0	—[c]	TA	40
				546	8.9	260		
				580	9.0	140		
			400	800	9.0	≤170	TL	This work
			425	513	—	195	FLUC	41
n-Heptane	—	0	400	800	8.7	≤200	TL	This work
n-Octane	—	0	500	550	9.0	350	TA	8
			1310[d]	550	9.0	—	TA	42
i-Octane	—	0	400	800	9.1	≤130	TL	This work
3-Methylpentane[e]	—	0	450	460	7.9	—	TA	43
				480	8.1			
				550	10.0			
Carbon disulfide	—	0	480	570	11	200	TA	44
Benzene	462[a]	0	397	570, 1000	9.0	360	TA	31
Toluene	463[b]	0.01	510	480	8.4	—	TA	45
Chloroform	462[a]	0.15	464	~960	—	168	TA	39
				~1020	—	178		
Dichloromethane	460[b]	0.22	490	475–750[f]	8.5	—	TA	46
Benzyl alcohol	470[b]	0.27	475	470–650	10.7	130	TA	32
Acetone	454	0.28	400	800	8.6	≤130	TL	This work
Ethanol	452[b]	0.29	490	475–750[f]	9.2	—	TA	46
			480	540	9.5	250	TA	44
			475	470–650	9.6	120	TA	32
Methanol	450[a]	0.31	490	481	9.0	—[c]	TA	40
				544	9.0	200		
				583	9.0	110		

[a] λ_{max} from ref. 37. [b] λ_{max} from ref. 38. [c] Instantaneous rise: time resolution of the experiments about 150 fs. [d] Data from 2-photon excitation of the S_1 state. [e] At 294 K. [f] Tunable range of the probe laser. [g] Detection technique: TA = transient absorption, TL = transient lens, FLUC = fluorescence upconversion.

(c) (3*R*,3′*R*)-Zeaxanthin. Time-resolved data for (3*R*,3′*R*)-zeaxanthin (conjugation: "9β2", Fig. 1) are somewhat more restricted,[40,56–59] and we therefore extended the database of τ_1 lifetimes to the solvents toluene, chloroform, acetone, and acetonitrile (Table 3). Our time constants for the $S_1 \rightarrow S_0$ internal conversion process are in the range between 9.3 and 10.4 ps, and no dependence on the solvent polarity is seen. In addition, we obtain good agreement for the solvents tetrahydrofuran, ethanol, and methanol, for which experimental τ_1 data from other groups are available. (3*R*,3′*R*)-Zeaxanthin shows almost the same behavior as β-carotene, and this is not unexpected because the conjugated systems of the two

Table 2 Lifetimes of lycopene in various organic solvents: $\tau_1(S_1 \rightarrow S_0)$ and $\tau_2(S_2 \rightarrow S_1)$

Solvent	λ_{max}/nm	Δf	λ_{pump}/nm	λ_{probe}/nm	τ_1/ps	τ_2/fs	Method[b]	Ref.
n-Hexane	—	0	510	500	4.9	—[a]	TA	40
				549	4.0	270		
				580	4.0	150		
			501	554	4.7	—	TA	50
			502	840–1040	4.1	20	TA	51
n-Hexane + 5% Benzene		0	501	400–700	3.9	380	TA	52
	471		400	800	3.1	≤170	TL	This work
n-Heptane	472	0	400	800	3.6	≤110	TL	This work
i-Octane	472	0	400	800	4.0	≤130	TL	This work
Cyclohexane	—	0	500–550	550–700	4.0	156	TA	53
Cyclohexene	480	0	400	800	3.9	≤180	TL	This work
Carbon disulfide	—	0	560	646	4.2	—	TA	54
Benzene	—	0	560	623	4.4	—	TA	54
Toluene	484	0.01	400	800	3.4	≤120	TL	This work
Chloroform	483	0.15	400	800	3.4	≤140	TL	This work
Tetrahydrofuran	479	0.21	400	800	3.6	≤170	TL	This work
Quinoline	—	—	560	646	3.8	—	TA	54
Nitrobenzene	—	—	560	634	3.7	—	TA	54
Pyridine	—	0.21	560	631	3.0	—	TA	54
Dimethylformamide	—	0.28	560	621	3.3	—	TA	54
Unspecified	—	—	—	—	3.8	—	TA	55

[a] Instantaneous rise: time resolution of the experiments about 150 fs. [b] Abbreviations see Table 1.

Table 3 Lifetimes of (3*R*,3′*R*)-zeaxanthin, (3*R*,3′*R*,6′*R*)-lutein, echinenone, canthaxanthin, and astaxanthin in various organic solvents: $\tau_1(S_1 \rightarrow S_0)$ and $\tau_2(S_2 \rightarrow S_1)$

Solvent	λ_{max}/nm	Δf	λ_{pump}/nm	λ_{probe}/nm	τ_1/ps	τ_2/fs	Method[c]	Ref.
(a) (3*R*,3′*R*)-Zeaxanthin								
n-Hexane	450	0	490	484	9.0	—[a]	TA	40
				547	9.6	270		
				577	9.0	200		
			420	512	9.0	—	TA	56
Toluene	463	0.01	400	800	9.7	≤270	TL	This work
Chloroform	462	0.15	400	800	10.3	≤230	TL	This work
Tetrahydrofuran		0.21	485	550	9.1	203	TA	57
				667	8.4	—		
	458		400	800	10.4	≤240	TL	This work
Acetone	453	0.28	400	800	9.4	≤190	TL	This work
Ethanol		0.29	485	560	9.3	250	TA	58
	452		400	800	9.8	≤220	TL	This work
Methanol		0.31	490	481	9.0	—[a]	TA	40
				548	9.1	280		
				579	9.0	120		
			490	1450	8.8	230	TA	59
				554	8.6	220		
	449		400	800	9.3	≤280	TL	This work
Acetonitrile	452	0.31	400	800	9.3	≤200	TL	This work
(b) (3*R*,3′*R*,6′*R*)-Lutein								
Toluene	457	0.01	400	800	15.3	≤180	TL	This work
Chloroform	456	0.15	400	800	15.1	≤120	TL	This work
Tetrahydrofuran	453	0.21	400	800	14.8	≤140	TL	This work
1-Octanol	—	0.23	1310[b]	550	15.0	—	TA	60
Dimethyl sulfoxide	462	0.26	400	800	14.3	≤120	TL	This work
Acetone	448	0.28	400	800	15.6	≤140	TL	This work
Ethanol	447	0.29	400	800	15.4	≤150	TL	This work
Acetonitrile	448	0.31	400	800	15.1	≤150	TL	This work
Methanol		0.31	490	555	15.0	—	TA	6
	444		400	800	14.3	≤160	TL	This work
Unspecified	—	—	—	—	14.6	—	TA	55
(c) Echinenone								
Toluene	472	0.01	400	800	7.5	≤160	TL	This work
Chloroform	473	0.15	400	800	7.9	≤180	TL	This work
Tetrahydrofuran	467	0.21	400	800	7.4	≤200	TL	This work
Acetone	456	0.28	400	800	8.1	≤150	TL	This work
(d) Canthaxanthin								
Toluene		0.01	510	480	5.2	—	TA	45
	470		400	800	4.9	≤160	TL	This work
Chloroform	470	0.15	400	800	5.1	≤140	TL	This work
Tetrahydrofuran	466	0.21	400	800	5.2	≤150	TL	This work
Acetone	460	0.28	400	800	4.9	≤140	TL	This work
Acetonitrile	460	0.31	400	800	5.1	—	TL	This work
(e) Astaxanthin								
CS_2	—	0	540	n.a.[d]	4.3	145	TA	17
Toluene	487	0.01	400	800	5.1	—	TL	This work
Chloroform	492	0.15	400	800	5.0	—	TL	This work
Tetrahydrofuran	482	0.21	400	800	5.5	—	TL	This work
Dimethyl sulfoxide	493	0.26	400	800	5.2	≤120	TL	This work
Acetone	478	0.28	400	800	5.2	≤120	TL	This work
Ethanol	479	0.29	400	800	5.1	—	TL	This work
Acetonitrile	476	0.31	500	n.a.[d]	4.9	165	TA	17
			400	800	4.9	—	TL	This work
Methanol	476	0.31	500	n.a.[d]	5.0	105	TA	17
			400	800	5.6	—	TL	This work
Unspecified	—	—	—	—	4.8	—	TA	55

[a] Instantaneous rise: time resolution of the experiments about 150 fs. [b] Data from 2-photon excitation of the S_1 state. [c] Abbreviations see Table 1. [d] Not applicable (global fitting).

carotenoids are identical (see below). On average our estimates of the lifetime τ_2 appear to be slightly larger than for β-carotene and lycopene.

(d) (3*R*,3′*R*,6′*R*)-Lutein. To our knowledge there are three measurements available for (3*R*,3′*R*,6′*R*)-lutein (conjugation: "9β1", Fig. 1), in methanol,[6] in 1-octanol,[60] and in an unspecified solvent.[55] These measurements yield values around 15 ps. We carried out experiments in seven additional solvents of different polarity. In general our time constants τ_1 are in excellent agreement with the earlier measurements, and we obtain values between 14.3 and 15.6 ps (Table 3). τ_2 is in the range of 150 fs.

We now turn to the three C_{40} carotenoids echinenone, canthaxanthin and astaxanthin, which contain carbonyl groups (Fig. 1). Their absorption spectra in different solvents are shown in Fig. 8. They are broad and do not show any clear three-peak structure. Only three very weak shoulders appear in the spectra of echinenone (A) and canthaxanthin (B, barely visible) around 490, 460 and 430 nm, and the astaxanthin spectrum (C) is structureless. This behavior is particularly evident for the solvent tetrahydrofuran. The loss of structure in the spectra of carbonyl carotenoids is usually explained by the influence of the conjugated electron-withdrawing C═O groups, which are thought to be responsible for a pronounced charge-transfer character of the excited states.[1] In addition, for astaxanthin, the presence of two hydroxyl groups might give rise to a broader distribution of conformers, which could explain the total loss of structure in the spectra.

(e) Echinenone. To our knowledge so far there have been no time-resolved pump–probe experiments carried out to investigate the IC processes in the C_{40} carbonyl carotenoid echinenone (conjugation: "9β2O1", Fig. 1). We performed measurements in the solvents toluene, chloroform, tetrahydrofuran and acetone, and find τ_1 values between 7.4 and 8.1 ps (Table 3), so there is no solvent-dependence. Our values are slightly larger than the 6.8, 6.4, and 6.2 ps determined by Polivka and co-workers for a related compound, 3′-hydroxyechinenone, in CS_2, *n*-hexane and methanol.[16] τ_2 values are limited by the finite time-resolution of our pump–probe-set up of approximately 150 fs. Again this in good agreement with the upper limits 135, 230 and 185 fs given by Polivka *et al.* for 3′-hydroxyechinenone in CS_2, *n*-hexane and methanol, respectively.[16]

(f) Canthaxanthin. Compared to echinenone, canthaxanthin has an additional conjugated C═O group in the second β-ionone ring, and the conjugation is thus "9β2O2" (Fig. 1). We observe a reduction of τ_1 compared to echinenone and typical values are between 4.9 and 5.2 ps (Table 3). Our value in the solvent toluene (4.9 ps) is in good agreement with the only earlier measurement of Wasielewski and Kispert (5.2 ps) using transient excited state absorption.[45] Upper limits for τ_2 are around 150 fs.

(g) Astaxanthin. Astaxanthin has the same type of conjugation as canthaxanthin ("9β2O2"), but differs by two additional OH groups on each ring, which are, however, not attached to the conjugated system (Fig. 1). We find basically the same τ_1 values as for canthaxanthin in toluene, chloroform, tetrahydrofuran, acetone and acetonitrile. Values vary between 4.9 and 5.6 ps (Table 3). Upper limits for τ_2 are about $\leq$120 fs. There are two earlier studies to compare with. The very recent TA experiments by Ilagan *et al.* in CS_2, acetonitrile and methanol as well as one earlier measurement by Frank *et al.* in an unspecified solvent are in good agreement with ours, with τ_1 being typically around 5 ps.[17,55]

5. Discussion

5.1 Dependence of τ_1 on conjugation length and substituents

The changes in τ_1 observed for the different carotenoids can be explained by variations in the conjugation length. Because the energy of the S_1 state decreases with increasing conjugation length, a simple "energy gap law model" would predict a decrease of the S_1 lifetime.[1,55,61,62] This is indeed observed. For instance, the τ_1 values for β-carotene (11 double bonds, "9β2") are around 9 ps (Table 1), whereas for (3*R*,3′*R*,6′*R*)-lutein (10 double bonds, "9β1") with one double bond less in one of the β-ionone rings the lifetime is roughly 15 ps (Table 3). This is in agreement with earlier results.[1] In the same way, for canthaxanthin (13 double bonds, "9β2O2", $\tau_1 \approx 5$ ps, Table 3), echinenone (12 double bonds, "9β2O1", $\tau_1 \approx 7.7$ ps, Table 3) and β-carotene (11 double bonds, "9β2", $\tau_1 \approx 9$ ps, Table 1), one finds a similar type of increase in τ_1. However, in this case the changes are smaller, because the conjugation of the carbonyl group is not as favorable, see below. This is directly reflected in the decay of the TL signals, as illustrated in Fig. 9.

For carotenoids with the same total conjugation length the observed changes of the S_1 lifetime can be explained by the deviation of the respective carotenoid structure from the C_{2h} symmetry of an "ideal" polyene. This leads to a decrease of the effective conjugation length, and thus an increase of τ_1.[1] For instance, lycopene, β-carotene and (3*R*,3′*R*)-zeaxanthin (Tables 1–3) have 11 conjugated double bonds. In the case of lycopene all double bonds are in plane ("11"), whereas for the other two carotenoids two of the double bonds are located in the terminal β-ionone rings ("9β2"). The latter ones are forced out-of-plane due to repulsion between methyl groups in the ring and hydrogen atoms on the conjugated backbone.[63–65] Therefore for lycopene values are around 3.5 ps, whereas for β-carotene and (3*R*,3′*R*)-zeaxanthin one obtains $\tau_1 = 9$–10 ps. By the same type of argument it is understandable that lycopene with its 11 "optimally" conjugated backbone double bonds still has a slightly shorter τ_1 time (3.5 ps) than canthaxanthin (5 ps) having 13 double bonds, of which, however, only 9 are optimally conjugated. In addition, carotenoids with C═O groups are known to have a shorter effective conjugation length compared to those containing a C═C group instead.[1] Finally, our data underline that substituents not attached to the conjugated system have no apparent influence on τ_1. This becomes clear when we compare the pairs β-carotene/(3*R*,3′*R*)-zeaxanthin (9–10 ps) and canthaxanthin/astaxanthin (each *ca.* 5 ps, Fig. 9), which differ by two hydroxyl groups located on the rings.

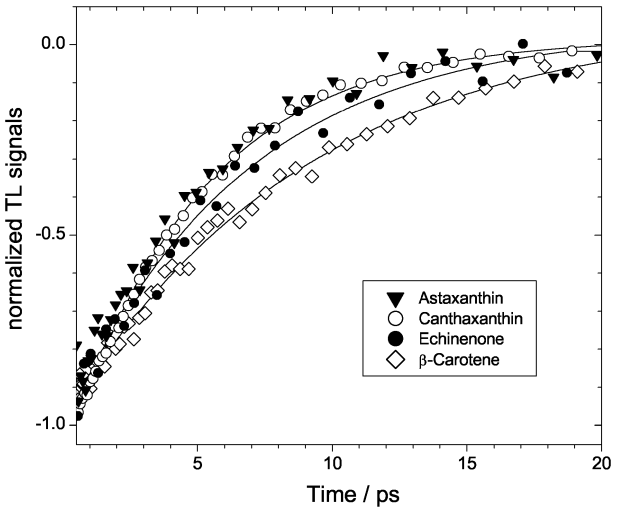

Fig. 9 Normalized TL signals for astaxanthin, canthaxanthin, echinenone, and β-carotene in acetone. Shown is only the part of each signal responsible for the time constant τ_1. Solid lines: best fit.

5.2 Influence of the solvent on τ_1

Our extensive solvent-dependent data show clearly that for the C_{40} carotenoids without a carbonyl group [lycopene, β-carotene, (3*R*,3′*R*)-zeaxanthin and (3*R*,3′*R*,6′*R*)-lutein] essentially no solvent effects on τ_1 are found, as underlined by the comparisons in Tables 1–3, covering a wide range from nonpolar solvents like *n*-hexane up to polar solvents like acetonitrile or methanol. No change is also observed for highly polarizable solvents like CS_2.

It is particularly interesting that the same is true for the C_{40} carbonyl carotenoids echinenone, canthaxanthin and astaxanthin investigated here (Table 3), and our echinenone data are in good agreement with measurements on 3′-hydroxyechinenone in different solvents by Polivka *et al.*[16] This is not necessarily expected *a priori* because several earlier reports for other carbonyl carotenoids showed dramatic effects. For instance, in peridinin the difference of τ_1 in nonpolar and polar media can reach a factor of 16.[13,14] These results were rationalized in terms of a combined S_1/ICT (intramolecular charge transfer) state, where a substantial transfer of electron density takes place in polar solvents. Indeed we have also observed in a separate systematic study on a series of apocarotenoids, that a substantial reduction of τ_1 is observed in polar media.[66] At the moment it is not clear, why echinenone, canthaxanthin and astaxanthin show no solvent dependent τ_1. The effect might be related to their relatively long conjugation length resulting in a S_0–S_1/ICT energy gap, which could make the S_0–S_1/ICT coupling strong enough, also in nonpolar environments.[67] Note, *e.g.*, that spheroidenone (conjugation "10O"), without terminal rings, also shows virtually no change in τ_1.[67,68]

6. Conclusions and outlook

In this paper we have demonstrated that transient lens spectroscopy is a convenient tool to study ultrafast IC processes in carotenoids. The method is experimentally simple, because it does not require a tunable probe wavelength, and has good sensitivity especially when coupled with high-frequency lock-in detection techniques. Some care must be exercised to quantify additional absorption contributions and solvent Kerr responses. This is, however, possible by a combination of "open-aperture" and "closed-aperture" pump–probe experiments with *Z*-scan measurements at fixed pump–probe delay times.

Our fits yield only upper limits for the time constant τ_2 of the IC process from S_2 to S_1. However, accurate time constants τ_1 for the $S_1 \rightarrow S_0$ internal conversion step can be extracted, which show a systematic increase with decreasing conjugation length, in good agreement with earlier studies. As far as the solvent dependence of τ_1 is concerned, it is interesting that the three related carbonyl carotenoids echinenone, canthaxanthin and astaxanthin are not sensitive to changes in solvent polarity. To extend our database of carbonyl containing species we are currently performing additional studies of the ultrafast IC dynamics of several apocarotenoids in various solvents.[66] These will hopefully shed more light on the special solvent-dependent intramolecular charge transfer processes operative in different carbonyl containing carotenoids.

Acknowledgements

The authors gratefully acknowledge financial support from the Alexander von Humboldt Foundation within the "Sofja Kovalevskaja Program" in the framework of the future investment program (Zukunftsinvestitionsprogramm, ZIP) of the German Federal Government. We thank J. Schroeder, D. Schwarzer, and A. I. Maergoiz for helpful discussions, and J. Zerbs and F. Ehlers for their experimental help. In addition, we would like to thank K. Luther and J. Troe for sharing their laser system for the TL experiments, as well as P. J. Walla for insightful comments. We are also particularly thankful to BASF AG, and here especially H. Ernst, for generously providing the highly purified *all-trans*-carotenoid samples and extensive discussions. Finally, we would like to thank T. Polivka for his advice in the very early stages of the experiments.

References

1 T. Polivka and V. Sundström, *Chem. Rev.*, 2004, **204**, 2021.
2 J. Koepke, X. Hu, C. Muenke, K. Schulten and H. Michel, *Structure*, 1996, **4**, 581.
3 R. Dellapenna, in *The Photochemistry of Carotenoids*, ed. H. A. Frank, A. J. Young, G. Britton and R. J. Cogdell, Kluwer, Dordrecht, The Netherlands, 1999, p. 21.
4 N. E. Holt, D. Zigmantas, L. Valkunas, X.-P. Li, K. K. Niyogi and G. R. Fleming, *Science*, 2005, **307**, 433.
5 R. Edge and T. G. Truscott, in *The Photochemistry of Carotenoids*, ed. H. A. Frank, A. J. Young, G. Britton and R. J. Cogdell, Kluwer, Dordrecht, The Netherlands, 1999, p. 223.
6 H. H. Billsten, P. Bhosale, A. Yemelyanov, P. S. Bernstein and T. Polivka, *Photochem. Photobiol.*, 2003, **78**, 138.
7 H. Ernst, *Pure Appl. Chem.*, 2002, **74**, 2213.
8 P. J. Walla, P. A. Linden, K. Ohta and G. R. Fleming, *J. Phys. Chem. A*, 2002, **106**, 1909.
9 M. Hilbert, A. Wehling, E. Schlodder and P. J. Walla, *J. Phys. Chem. B*, 2004, **108**, 13022.
10 P. Kukura, D. W. McCamant and R. A. Mathies, *J. Phys. Chem. A*, 2004, **108**, 5921.
11 G. Cerullo, D. Polli, G. Lanzani, S. De Silvestri, H. Hashimoto and R. J. Cogdell, *Science*, 2002, **298**, 2395.
12 R. G. Hiller, in *The Photochemistry of Carotenoids*, ed. H. A. Frank, A. J. Young, G. Britton and R. J. Cogdell, Kluwer, Dordrecht, The Netherlands, 1999, p. 81.
13 J. A. Bautista, R. E. Connors, B. B. Raju, R. G. Hiller, F. P. Sharples, D. Gosztola, M. R. Wasielewski and H. A. Frank, *J. Phys. Chem. A*, 1999, **103**, 8751.
14 J. A. Bautista, R. G. Hiller, F. P. Sharples, D. Gosztola, M. R. Wasielewski and H. A. Frank, *J. Phys. Chem. A*, 1999, **103**, 2267.
15 D. Zigmantas, R. G. Hiller, A. Yartsev, V. Sundström and T. Polivka, *J. Phys. Chem. B*, 2003, **107**, 5339.
16 T. Polivka, C. A. Kerfeld, T. Pascher and V. Sundström, *Biochemistry*, 2005, **44**, 3994.
17 R. P. Ilagan, R. L. Christensen, T. W. Chapp, G. N. Gibson, T. Pascher, T. Polivka and H. A. Frank, *J. Phys. Chem. A*, 2005, **109**, 3120.
18 S. Krawczyk and G. Britton, *Biochim. Biophys. Acta*, 2001, **1544**, 301.
19 A. A. C. van Wijk, A. Spaans, N. Uzunbajakava, C. Otto, H. J. M. de Groot, J. Lugtenburg and F. Buda, *J. Am. Chem. Soc.*, 2005, **127**, 1438.
20 M. Cianci, P. J. Rizkallah, A. Olczak, J. Raftery, N. E. Chayen, P. F. Zagalsky and J. R. Helliwell, *Proc. Natl. Acad. Sci.*, 2002, **99**, 9795.
21 C. A. Kerfeld, M. R. Sawaya, V. Brahmandam, D. Cascio, K. K. Ho, C. C. Trevithick-Sutton, D. W. Krogmann and T. O. Yeates, *Structure*, 2003, **11**, 55.
22 K. Ito, M. Mutoh, A. Harata and T. Sawada, *Chem. Phys. Lett.*, 1997, **275**, 349.
23 T. Berthoud, N. Delorme and P. Mauchien, *Anal. Chem.*, 1985, **57**, 1216.
24 M. Sheik-Bahae, A. A. Said and E. W. Van Stryland, *Opt. Lett.*, 1989, **14**, 955.
25 M. Sheik-Bahae, A. A. Said, T. H. Wei, D. J. Hagan and E. W. Van Stryland, *IEEE J. Quant. Electron.*, 1990, **26**, 760.
26 M. Terazima, *Isr. J. Chem.*, 1998, **38**, 143.
27 M. Franko and C. D. Tran, *Rev. Sci. Instrum.*, 1996, **67**, 1.
28 P. Cong, Y. J. Chang and J. D. Simon, *J. Phys Chem.*, 1996, **100**, 8613.
29 M. Terazima, *Opt. Lett.*, 1995, **20**, 25.
30 M. Ricci, R. Torre, P. Foggi, V. Kamalov and R. Righini, *J. Chem. Phys.*, 1995, **102**, 9537.
31 M. Yoshizawa, H. Aoki, M. Ue and H. Hashimoto, *Phys. Rev. B*, 2003, **67**, 174302.
32 F. L. de Weerd, I. H. M. van Stokkum and R. van Grondelle, *Chem. Phys. Lett.*, 2002, **354**, 38.
33 M. Sheik-Bahae, J. Wang, R. DeSalvo, D. J. Hagan and E. W. Van Stryland, *Opt. Lett.*, 1992, **17**, 258.
34 J. Wang, M. Sheik-Bahae, A. A. Said, D. J. Hagan and E. W. Van Stryland, *J. Opt. Soc. Am. B*, 1994, **11**, 1009.

35 O. V. Przhonska, J. H. Lim, D. J. Hagan, E. W. Van Stryland, M. V. Bondar and Y. L. Slominsky, *J. Opt. Soc. Am. B*, 1998, **15**, 802.
36 J. H. Lim, O. V. Przhonska, S. Khodja, S. Yang, T. S. Ross, D. J. Hagan, E. W. Van Stryland, M. V. Bondar and Y. L. Slominsky, *Chem. Phys.*, 1999, **245**, 79.
37 N. E. Craft and J. H. Soares Jr., *J. Agric. Food Chem.*, 1992, **40**, 431.
38 A. N. Macpherson and T. Gillbro, *J. Phys. Chem. A*, 1998, **102**, 5049.
39 J.-P. Zhang, L. H. Skibsted, R. Fujii and Y. Koyama, *Photochem. Photobiol.*, 2001, **73**, 219.
40 H. H. Billsten, D. Zigmantas, V. Sundström and T. Polivka, *Chem. Phys. Lett.*, 2002, **355**, 465.
41 H. Kandori, H. Sasabe and M. Mimuro, *J. Am. Chem. Soc.*, 1994, **116**, 2671.
42 P. J. Walla, P. A. Linden, C.-P. Hsu, G. D. Scholes and G. R. Fleming, *Proc. Natl. Acad. Sci.*, 2000, **97**, 10808.
43 M. R. Wasielewski, D. G. Johnson, E. G. Bradford and L. D. Kispert, *J. Chem. Phys.*, 1989, **91**, 6691.
44 A. P. Shreve, J. K. Trautman, T. G. Owens and A. C. Albrecht, *Chem. Phys. Lett.*, 1991, **178**, 89.
45 M. R. Wasielewski and L. D. Kispert, *Chem. Phys. Lett.*, 1986, **128**, 238.
46 Z. He, L. D. Kispert, R. M. Metzger, D. Gosztola and M. R. Wasielewski, *J. Phys. Chem. B*, 2000, **104**, 6302.
47 T. Siebert, M. Schmitt, V. Engel, A. Materny and W. Kiefer, *J. Am. Chem. Soc.*, 2002, **124**, 6242.
48 T. Siebert, R. Maksimenka, A. Materny, V. Engel, W. Kiefer and M. Schmitt, *J. Raman Spectrosc.*, 2002, **33**, 844.
49 B. Valeur, *Molecular Fluorescence - Principles and Applications*, Wiley-VCH, Weinheim, 2002.
50 J.-P. Zhang, R. Fujii, P. Qian, T. Inaba, T. Mizoguchi, Y. Koyama, K. Onaka and Y. Watanabe, *J. Phys. Chem. B*, 2000, **104**, 3683.
51 R. Fujii, T. Inaba, Y. Watanabe, Y. Koyama and J.-P. Zhang, *Chem. Phys. Lett.*, 2003, **369**, 165.
52 F. S. Rondonuwu, Y. Watanabe, R. Fujii and Y. Koyama, *Chem. Phys. Lett.*, 2003, **376**, 292.
53 D. Polli, G. Cerullo, G. Lanzani, S. De Silvestri, H. Hashimoto and R. J. Cogdell, *Synth. Met.*, 2003, **139**, 893.
54 J.-P. Zhang, C.-H. Chen, Y. Koyama and H. Nagae, *J. Phys. Chem. B*, 1998, **102**, 1632.
55 H. A. Frank, V. Chynwat, R. Z. B. Desamero, R. Farhoosh, J. Erickson and J. Bautista, *Pure Appl. Chem.*, 1997, **69**, 2117.
56 H. A. Frank, A. Cua, V. Chynwat, A. Young, D. Gosztola and M. R. Wasielewski, *Photosynth. Res.*, 1994, **41**, 389.
57 M. P. Debreczeny, M. R. Wasielewski, S. Shinoda and A. Osuka, *J. Am. Chem. Soc.*, 1997, **119**, 6407.
58 H. H. Billsten, V. Sundström and T. Polivka, *J. Phys. Chem. A*, 2005, **109**, 1521.
59 T. Polivka, J. L. Herek, D. Zigmantas, H. Akerlund and V. Sundström, *Proc. Natl. Acad. Sci.*, 1999, **96**, 4914.
60 P. J. Walla, P. A. Linden and G. R. Fleming, in *Ultrafast Phenomena*, ed. T. Elsaesser, S. Mukamel, M. M. Murnane and N. F. Scherer, Springer, New York, 2000, p. 671.
61 R. Englman and J. Jortner, *Mol. Phys.*, 1970, **18**, 145.
62 V. Chynwat and H. A. Frank, *Chem. Phys.*, 1995, **194**, 237.
63 R. L. Christensen, M. Goyette, L. Gallagher, J. Duncan, B. DeCoster, J. Lugtenburg, F. J. Jansen and I. van der Hoef, *J. Phys. Chem. A*, 1999, **103**, 2399.
64 R. L. Christensen and B. E. Kohler, *Photochem. Photobiol.*, 1973, **18**, 293.
65 R. Hemley and B. E. Kohler, *Biophys. J.*, 1977, **20**, 377.
66 T. Lenzer, K. Oum, J. Seehusen and M. T. Seidel, in preparation.
67 D. Zigmantas, R. G. Hiller, F. P. Sharples, H. A. Frank, V. Sundström and T. Polivka, *Phys. Chem. Chem. Phys.*, 2004, **6**, 3009.
68 H. A. Frank, J. A. Bautista, J. Josue, Z. Pendon, R. G. Hiller, F. P. Sharples, D. Gosztola and M. R. Wasielewski, *J. Phys. Chem. B*, 2000, **104**, 4569.